

# Multi-Granularity Class Prototype Topology Distillation for Class-Incremental Source-Free Unsupervised Domain Adaptation

Peihua Deng<sup>1</sup> Jiehua Zhang<sup>2</sup> Xichun Sheng<sup>3</sup> Chenggang Yan<sup>1</sup>  
Yaoqi Sun<sup>1</sup> Ying Fu<sup>4</sup> Liang Li<sup>5</sup>

<sup>1</sup>Hangzhou Dianzi University, Hangzhou, Zhejiang, China

<sup>2</sup>Xi'an Jiaotong University, Xi'an, Shaanxi, China

<sup>3</sup>Macao Polytechnic University, Macao, China

<sup>4</sup>School of Computer Science and Technology, Beijing Institute of Technology, Beijing, China

<sup>5</sup>Institute of Computing Technology, Chinese Academy of Sciences, Beijing, China

## Abstract

This paper explores the Class-Incremental Source-Free Unsupervised Domain Adaptation (CI-SFUDA) problem, where the unlabeled target data come incrementally without access to labeled source instances. This problem poses two challenges, the disturbances of similar source-class knowledge to target-class representation learning and the new target knowledge to old ones. To address them, we propose the Multi-Granularity Class Prototype Topology Distillation (GROTO) algorithm, which effectively transfers the source knowledge to the unlabeled class-incremental target domain. Concretely, we design the multi-granularity class prototype self-organization module and prototype topology distillation module. Firstly, the positive classes are mined by modeling two accumulation distributions. Then, we generate reliable pseudo-labels by introducing multi-granularity class prototypes, and use them to promote the positive-class target feature self-organization. Secondly, the positive-class prototypes are leveraged to construct the topological structures of source and target feature spaces. Then, we perform the topology distillation to continually mitigate the interferences of new target knowledge to old ones. Extensive experiments demonstrate that our proposed method achieves state-of-the-art performances on three public datasets.

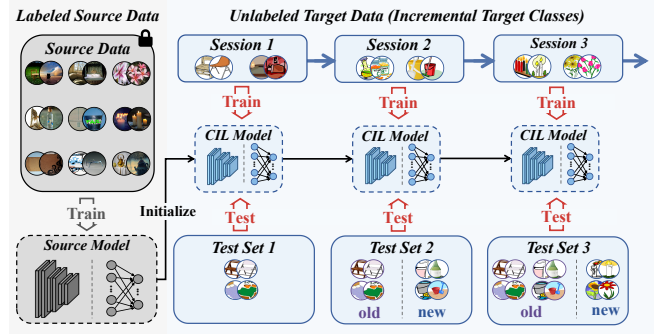


Figure 1: An illustration of Class-Incremental Source-Free Unsupervised Domain Adaptation (CI-SFUDA), where the labeled source data contain all classes while the unlabeled target data come incrementally without access to source instances, and the previously learned target data are unavailable for later adaptations.

class prototypes. However, these works are established on the identical label space assumption between source and target domains. In practice, the model often trains on a large-scale labeled dataset and then transfers knowledge to the small unlabeled target domain [1, 2]. In such a nonidentical label space scenario, traditional SFUDA methods may push the unlabeled target data toward similar source-class clusters outside the target label space. The latest source-free universal domain adaptation (SF-UniDA) works have mitigated the problem through the feature clustering and feature decomposition methods [23, 24, 30], but they assume the availability of all the target data in advance. In the dynamic changing environment, target data of all the classes cannot be easily collected at once, while they always come in a stream of different classes [21, 18]. In such a case, existing methods require training from scratch when new data arrive, consuming substantial time and storage resources. Furthermore, previously learned data may be unavailable for data privacy issues. Therefore, the pre-trained source model is expected to adapt to new tar-

## 1 Introduction

Unsupervised Domain Adaptation (UDA) [4, 20, 26] relies on labeled source data and unlabeled target data to mitigate the domain gap. But in some practical applications, it is infeasible to access source data when training on the target domain, while only the pre-trained source model and unlabeled target data are provided, known as Source-Free Unsupervised Domain Adaptation (SFUDA) [22, 12, 3].

To facilitate the knowledge transfer, most SFUDA methods adapt target distributions with the self-training strategy, where pseudo-labels are generated by a non-parameter classifier based on the similarity between image features and the

get classes while maintaining the old knowledge without re-training [14, 18].

In this paper, we explore the *Class-Incremental Source-Free Unsupervised Domain Adaptation* (CI-SFUDA) problem, where the target data come incrementally as sequential sessions without available source instances, while the target classes of each session derive from the subset of the source label space as shown in Figure 1. Therefore, CI-SFUDA has two challenges: (1) the disturbance of similar source-class knowledge for target-class representation learning. Due to the label space of the target domain at each session only occupying a subspace of the source one, unlabeled target data may be misassigned pseudo-labels from similar source classes outside the session, leading to biased target representations. (2) The shocks of new target knowledge to old ones. When adapting to new classes, the optimizer updates model weights to adjust towards the features and patterns of new classes, leading to the forgetting of old knowledge. This indicates that the model needs to ensure consistency of the source semantic knowledge learned from all classes and the target semantic knowledge gradually accumulated across multiple sessions.

To address them, we propose the Multi-Granularity Class **PRO**typology **TO**pology Distillation (GROTO) algorithm, which aims to continually adapt the source model to different incremental target sessions. Firstly, we design the multi-granularity class prototype self-organization module to mitigate the bias caused by similar source-class knowledge in the representation learning of new target classes. Specifically, we introduce the hybrid knowledge-driven positive class mining strategy with the accumulation distributions of source similarity and target probability at each session. Then, we generate pseudo-labels for target data by introducing the multi-granularity class prototypes, which effectively alleviates the disturbance of noisy labels for hard-transfer data. With the reliable pseudo-labels, we perform the target feature self-organization to pull same-class features closer and push features of different classes farther apart.

Secondly, we propose the prototype topology distillation module to continually reduce the shocks of new target knowledge to old ones. In detail, we compute the positive-class prototypes to construct the topological structures of feature spaces for source and target domains. Then, we perform the point-to-point distillation based on the source and incremental target topological structures. It enables the model to continually adapt to multiple sessions, while maintaining consistency of the learned target knowledge and the corresponding source ones, thus reducing the disturbance of new target classes to old ones.

Experiments on three benchmark datasets show that our method outperforms the state-of-the-art methods. In summary, the main contributions of this paper are as follows:

- We explore the class-incremental source-free unsupervised domain adaptation (CI-SFUDA) problem, and propose the multi-granularity class prototype topology distillation (GROTO) algorithm.
- We design the multi-granularity class prototype self-

organization module to mitigate the interference from similar source-class knowledge to the target-class representation learning.

- We design the prototype topology distillation module to mitigate the shocks of new target knowledge to old ones.

## 2 Related Work

**Source-free Unsupervised Domain Adaptation (SFUDA).** SFUDA transfer the pre-trained source model to the unlabeled target domain [16, 12, 3]. BMD [22] uses the multicentric dynamic prototype method to enhance the diversity of feature prototypes and then generate robust pseudo-labels, while the number of empirical prototypes is fixed and always different in the various datasets. Recent self-training framework methods [12, 3] introduce curriculum learning or contrastive learning to filter and handle the noisy pseudo-labels on the target domain. However, these methods fail to transfer the model from a large-scale dataset to a small-scale one.

**Source-free Universal Domain Adaptation (SF-UniDA).** The SF-UniDA task largely addresses adapting source models trained on large-scale datasets to small unlabeled datasets under source-free conditions [17, 23, 24]. Previous works minimize the influences of irrelevant classes on the target domain with fixed threshold-based methods. Recently, representation-based methods become popular. GLC [23] uses clustering strategies to distinguish domain-public and domain-private data. Some works use statistical distribution-based or causality-driven feature decomposition methods [24, 30] to reduce disturbance from irrelevant information in the features. However, the target data usually come incrementally in practice. In such a scenario, these SF-UniDA methods struggle to well achieve continual adaptation, while GROTO can effectively address it.

**Class-Incremental Learning (CIL).** CIL [32, 7, 8] faces a scenario where the classes arrive incrementally as sequential sessions, and the previously learned data are no longer unavailable at new sessions. The non-memory methods solve it by altering network structures or optimizing parameters to deal with the new tasks [35, 8, 10]. The memory-based methods store the selected exemplars of previous tasks and perform memory replay by knowledge distillation in the current task [11, 7], thus mitigating the catastrophic forgetting problem [25, 34].

## 3 Proposed Method

### 3.1 Problem Formulation

Let  $\mathcal{D}_s = \{(x_j^s, y_j^s) | y_j^s \in Y^s\}_{j=1}^{n_s}$  denotes the source domain with  $n_s$  source data, where  $Y^s$  is the source label set and the number of source classes is  $|Y^s| = K$ . We need to adapt the source model  $M_s$  to the sequential training datasets  $D^1, D^2, \dots, D^t, D^{t+1}$ , and build a unified target model  $M_t$ , where  $D^t = \{(x_i)\}_{i=1}^{n_t}$  is the unlabeled target domain of the

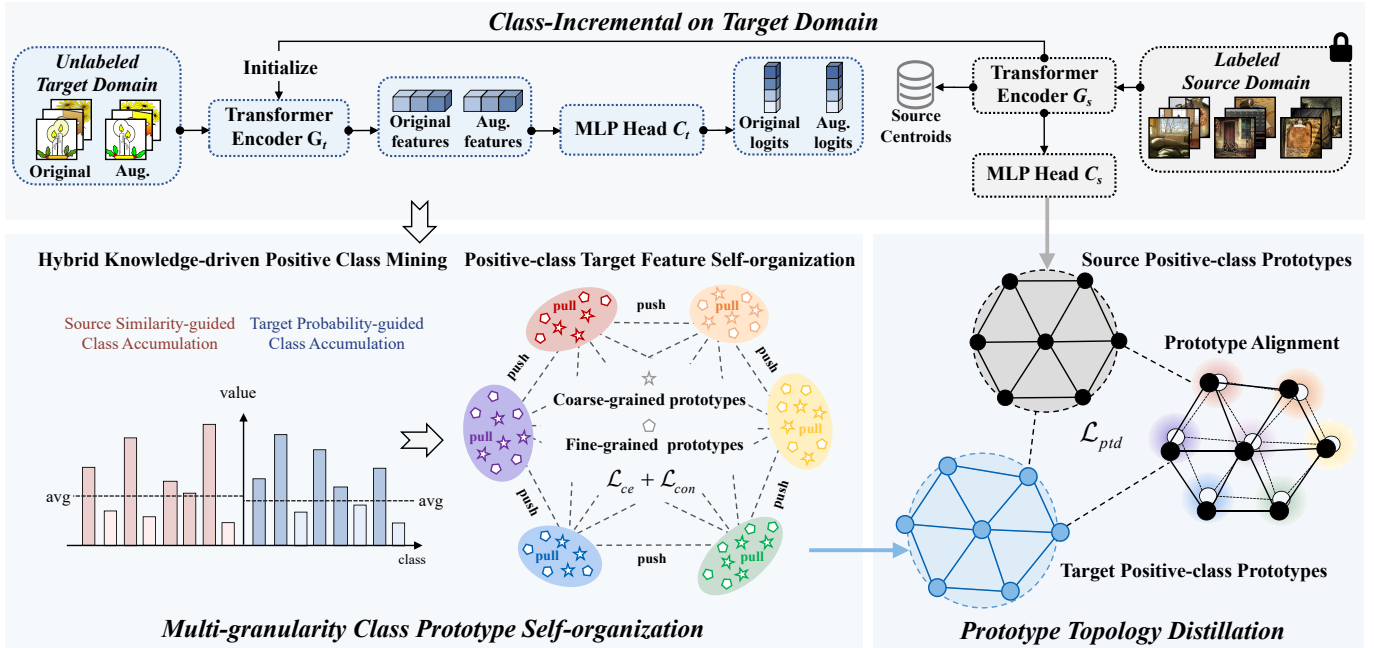


Figure 2: An overview of the GROTO algorithm, it includes two modules: 1) Multi-granularity class prototype self-organization: we mine the positive classes by modeling the source similarity and target probability accumulation distributions, and then promote the positive-class target features self-organization based on the multi-granularity class prototypes via  $\mathcal{L}_{ce}$  and  $\mathcal{L}_{con}$ . 2) Prototype topology distillation: we compute the positive-class prototypes to align the topological structures of source and target feature spaces via  $\mathcal{L}_{ptd}$ .

$t$ -th session with  $n_t$  samples,  $G_t$  and  $C_t$  are the feature extractor and classifier of  $M_t$ ,  $G_s$  and  $C_s$  are the feature extractor and classifier of  $M_s$ .  $Y^p$  and  $Y^q$  are disjoint target label sets at the  $p$ -th and  $q$ -th target sessions, *s.t.*  $\forall p \neq q, Y^p \cap Y^q = \emptyset$ . Moreover,  $Y^t$  at each session  $t$  is a subset of the source label set, *i.e.*  $Y^t \subset Y^s$ . At session  $t + 1$ , the target model  $M_t$  is learned from  $D^{t+1}$  without the old-class training sets  $D^1, D^2, \dots, D^t$ . Then,  $M_t$  is evaluated on the concatenated set of all the seen sets  $\bigcup_{i=1}^{t+1} D^i$ .

## 3.2 Overall Framework

The overview of GROTO is shown in Figure 2. **Firstly**, to reduce the disturbances of similar source-class knowledge in the target-class representation learning, we develop the multi-granularity class prototype self-organization module, which identifies cross-domain shared positive classes and conducts target feature self-organization. In detail, we mine the positive classes of new sessions by modeling the source similarity and the target probability accumulation distributions. Then, we generate the pseudo-labels for target data by identifying the coarse-grained and fine-grained class prototypes. With these reliable pseudo-labels, we conduct the target feature self-organization with the cross-entropy loss  $\mathcal{L}_{ce}$  and contrastive loss  $\mathcal{L}_{con}$ . **Secondly**, to continually mitigate the disturbances of new target knowledge to old ones, we propose the prototype topology distillation module. We compute the

positive-class prototypes to construct the topological structures of feature spaces, then perform the point-to-point distillation between the source and target topological structures via the topology distillation loss  $\mathcal{L}_{ptd}$ .

## 3.3 Multi-granularity Class Prototype Self-organization

A mainstream paradigm of solving SFUDA is the self-training strategy, which assigns pseudo labels to unlabeled target data and learns from them. However, when the target data comes incrementally, its label set  $Y^t$  at the  $t$ -th session is a subset of the source label set  $Y^s$ . Incorrect pseudo-labels out of  $Y^t$  may be assigned to unlabeled target data in the training set  $D^t$  of the  $t$ -th session, resulting in target features being closer to similar source-class clusters outside the target label space of each session. To solve this problem, we propose the multi-granularity class prototype self-organization module that consists of two steps: 1) hybrid knowledge-driven positive class mining (HKPCM), 2) positive-class target feature self-organization (PTFS).

**Hybrid Knowledge-driven Positive Class Mining.** In CI-SFUDA, since the target classes of different sessions are non-overlapping subsets of the source label space, we designate the classes within the new-session label space as positive classes (*e.g.*  $Y^t$  at the  $t$ -th session), and the remaining classes as negative classes.

To identify positive classes, the hybrid knowledge-driven positive class mining strategy with the accumulation distributions of source similarity and target probability is proposed. Specifically, for the source similarity-guided class accumulation distributions, we first load the stored source feature centroids  $s = [s_1, \dots, s_K]$  of all the source classes  $K$ . Next, we use the source feature extractor  $G_s$  to generate features  $g = [g_1, \dots, g_{n_t}]$  for  $n_t$  target data at the  $t$ -th session, and calculate the similarity matrix  $R \in \mathbb{R}^{n_t \times K}$  by:

$$R = g^T \cdot s, \quad (1)$$

where each element  $r_{ij} \in R$  represents the similarity between the  $i$ -th target data and the  $j$ -th source centroid. We normalize  $r_{ij}$  with the softmax normalization and compute the average similarity  $S_k$  for each source class  $k$ . Then, we identify the positive classes by  $S_k > \frac{1}{K} \sum_{j=1}^K S_j$ , as shown in the red histogram in Figure 2.

For the target probability-guided class accumulation distributions, we generate the prediction for each target data  $x_i$  of the  $t$ -th session to obtain the cumulative probability  $P_k$  for each source class  $k$  in  $Y^s$ :

$$P_k = \sum_{i=1}^{n_t} C_s(G_s(x_i)). \quad (2)$$

We normalize the cumulative predicted probability  $P_k$  of each source class  $k$  with the min-max normalization and identify the positive classes by  $P_k > \frac{1}{K} \sum_{j=1}^K P_j$ , as shown in the blue histogram in Figure 2.

With the pseudo label assigned in subsequent stages, unique pseudo-labels evolve as positive classes.

**Positive-class Target Feature Self-organization.** To generate reliable pseudo-labels, we first identify the coarse-grained and fine-grained prototypes. Then we conduct target feature self-organization via the cross-entropy loss and contrastive loss to make the intra-class features more compact and inter-class features more separable.

*Coarse-grained prototypes*  $O_c$  include the source and target coarse-grained ones of positive classes. The source classifier weights  $\mu = [\mu_1, \dots, \mu_N]$  of  $N$  positive classes are considered as the source coarse-grained prototypes, which denote the stable convergence points of each positive class on the source domain. Further, considering the domain gap, we identify target coarse-grained prototypes to provide the representation of target-class central tendencies, which are representative data with high similarity to target feature centroids of positive classes. In detail, for each positive class  $n$ , the class centroid  $c_n$  is calculated by averaging features with the same initial pseudo-label  $\arg \max_n C_t(G_t(x_i)) = n$  by:

$$c_n = \frac{1}{|S_n|} \sum_{x_n \in S_n} G_t(x_n), \quad (3)$$

where  $S_n$  is the set of all the target data that pseudo-label is  $n$ ,  $x_n$  is the data in  $S_n$ . For each data  $x_n$ , we calculate its cosine distance with  $c_n$  by  $d(x_n, c_n) = 1 - \frac{G_t(x_n) \cdot c_n}{\|G_t(x_n)\|_2 \|c_n\|_2}$ ,

and compute the average cosine distance of all the data with initial pseudo label  $n$  as the threshold  $\tau_s$ :

$$\tau_s = \frac{1}{|S_n|} \sum_{x_n \in S_n} d(x_n, c_n). \quad (4)$$

We identify the features of  $x_n$  as target coarse-grained prototypes of positive class  $n$  by  $d(x_n, c_n) < \tau_s$ .

*Fine-grained prototypes*  $O_f$  are the target features with reliable initial pseudo-labels, which provide detailed representations about each target class. To select the fine-grained prototypes, we first conduct general data augmentation to simulate the distribution offsets. Then we calculate the uncertainty  $u_i$  of the prediction confidences (*conf*) for each target data  $x_i$  and its augmented data  $x'_i$  of the  $t$ -th session by taking the standard deviation (*std*):

$$u_i = \text{std}(\text{conf}(x_i), \text{conf}(x'_i)). \quad (5)$$

The thresholds  $\tau_c$  and  $\tau_u$  are computed as:

$$\tau_c = \frac{1}{2n_t} \sum_{i=1}^{n_t} (\text{conf}(x_i) + \text{conf}(x'_i)), \quad \tau_u = \frac{1}{n_t} \sum_{i=1}^{n_t} u_i. \quad (6)$$

The feature of  $x_i$  is considered one of the fine-grained prototypes  $O_f$  by:

$$\text{conf}_{\text{avg}}(x_i, x'_i) > \tau_c \quad \text{and} \quad u_i < \tau_u, \quad (7)$$

where  $\text{conf}_{\text{avg}}$  is the average prediction confidence of the data pair.

Let  $O = O_c \cup O_f$  be the union of all the coarse-grained and fine-grained prototypes, and  $o_n \in O$  be the prototypes of each positive class  $n$ . We compute the average of the cosine distances from each of the remaining target data  $x_j$  to all the  $n$ -th positive-class prototypes  $o_n$  as the distance of  $x_j$  to the  $n$ -th positive-class  $D(x_j, n)$ . Then, we assign the pseudo-label  $\bar{y}_j$  to  $x_j$ :

$$\bar{y}_j = \arg \min_n D(x_j, n). \quad (8)$$

Finally, we conduct target feature self-organization with the cross-entropy loss and unsupervised contrastive learning [13]:

$$\mathcal{L}_{ce} = -\frac{1}{B} \sum_{i=1}^B \bar{y}_i \cdot \log C_t(G_t(x_i)), \quad (9)$$

$$\mathcal{L}_{con} = \frac{1}{2B} \sum_{b=1}^{2B} [\ell_{2b-1, 2b} + \ell_{2b, 2b-1}], \quad (10)$$

$$\ell_{i,j} = -\log \frac{\exp(\phi(G_t(x_i), G_t(x'_i))/\kappa)}{\sum_{b=1}^{2B} \mathbb{1}_{b \neq i} \exp(\phi(G_t(x_i), G_t(x'_i))/\kappa)}, \quad (11)$$

$$\mathcal{L}_{ptfs} = \mathcal{L}_{ce} + \mathcal{L}_{con}, \quad (12)$$

where  $B$  is the batch size,  $\bar{y}_i$  is the pseudo label of  $x_i$ ,  $\kappa$  is the temperature constant and  $\phi(\cdot, \cdot)$  is the cosine similarity. By combining  $\mathcal{L}_{con}$  and  $\mathcal{L}_{ce}$  (denoted as  $\mathcal{L}_{ptfs}$ ), we can make the embedding space more compact while preserving the fine-grained information about the decision boundary of each target class.



### 3.4 Prototype Topology Distillation

At a new incremental session, the optimizer updates model weights to adjust towards the features and patterns of new classes, leading to the forgetting of old knowledge. ProCA [18] mitigates this problem by the knowledge replay strategy. They construct a memory bank  $\mathcal{M} = \{(m_i, \hat{y}_i, \bar{y}_i)\}_{i=1}^{N_r}$  to store a small number of representative exemplars for replaying all  $N'$  existing positive classes, where  $m_i, \hat{y}_i, \bar{y}_i$  and  $N_r$  respectively denote the exemplar, soft prediction, pseudo-label and the number of all exemplars. For each existing class  $n'$  in the memory bank,  $n_r$  exemplars are stored, where  $n_r = N_r/N'$ . This paper also maintains a similar memory bank. To make it compatible with the HKPCM module, we only store the one with higher confidence in  $\mathcal{M}$ , if a positive class is identified in multiple sessions. We perform the exemplar replay [34] by:

$$\mathcal{L}_{rep} = -\frac{1}{N_r} \sum_{i=1}^{N_r} \hat{y}_i^\top \log C_t(G_t(m_i)), \quad (13)$$

where  $C_t(G_t(m_i))$  is the prediction of the exemplar  $m_i$  at the new session.

Due to the insufficient knowledge distillation and data imbalance between old and new classes ( $N_r \ll n_t$ ), relying only on the exemplar memory replay strategy results in the decision boundary overfitting to the dominant new classes [5, 15]. In CI-SFUDA, the source model is trained on labeled data of all the classes at once, acquiring semantic knowledge from all classes. This indicates that the model needs to ensure consistency between the source semantic knowledge learned from all classes and the target semantic knowledge gradually accumulated across multiple sessions.

In light of this, we propose the prototype topology distillation (PTD) module, which continually reduces the shocks of new target knowledge to old ones. During the target incremental training process, we use the source topological structure to prospectively support the decision boundary construction of new and old classes at each session. In detail, we first adopt classifier weights of the source and target model as source prototypes  $\mu = [\mu_1, \dots, \mu_N]$  and the target ones  $f = [f_1, \dots, f_N]$  to construct the topological structures of feature spaces for  $N$  positive classes. As the target prototypes tend to be moved towards the neighboring source prototypes with the same label, we design the compactness loss  $\mathcal{L}_{com}$ :

$$\mathcal{L}_{com} = \frac{1}{N} \sum_{j=1}^N \sum_{i=1}^N d(\mu_i, f_j^T) \frac{p(f_i) \exp(\mu_i f_j^T)}{\sum_{i'=1}^N p(f_{i'}) \exp(\mu_{i'} f_j^T)}, \quad (14)$$

where  $p(\cdot)$  is the target proportion. The unnormalized likelihood term  $\exp(\mu_i f_j^T)$  measures the similarity of the  $i$ -th source and  $j$ -th target prototypes. The cosine distance  $d(\cdot, \cdot)$  is considered to be the distillation cost to adjust the target prototypes. Minimizing  $\mathcal{L}_{com}$  encourages each target prototype to be closer to the neighboring source prototype with the same label, thus enhancing the intra-class compactness between domains.

Further, we also design the separability loss  $\mathcal{L}_{sep}$ :

$$\mathcal{L}_{sep} = \sum_{i=1}^N p(f_i) \sum_{j=1}^N d(\mu_i, f_j^T) \frac{\exp(\mu_i f_j^T)}{\sum_{j'=1}^N \exp(\mu_i f_{j'}^T)}, \quad (15)$$

where  $\frac{\exp(\mu_i f_j^T)}{\sum_{j'=1}^N \exp(\mu_i f_{j'}^T)}$  normalizes the probabilities across the target prototypes for each source prototype. This operation ensures that each source prototype can be aligned to the corresponding target one. Minimizing  $\mathcal{L}_{sep}$  reduces the mismatch risk of cross-domain prototypes, thereby promoting the separability of inter-class prototypes.

Finally, combining the compactness loss  $\mathcal{L}_{com}$  and separability loss  $\mathcal{L}_{sep}$ , our point-to-point prototype topology distillation loss  $\mathcal{L}_{ptd}$  is expressed as:

$$\mathcal{L}_{ptd} = \mathcal{L}_{com} + \mathcal{L}_{sep}. \quad (16)$$

$\mathcal{L}_{ptd}$  mitigates the decision boundary overfitting to new classes at each session, thereby reducing the cost of maintaining old-class knowledge on the later adaptations.

## 4 Experiment

### 4.1 Experimental Setup

**Dataset.** We conduct experiments on the variants of three benchmark datasets, *i.e.*, Office-31 [28], Office-Home [33] and ImageNet-Caltech [27, 9]. 1) **Office-31-CI** contains three domains with shared 31 classes in the office environment, *i.e.*, Amazon (A), DSLR (D), and Webcam (W). Each domain is divided into three disjoint subsets with 10 classes for each in alphabetical order. 2) **Office-Home-CI** divides images of everyday objects into four domains with shared 65 classes, *i.e.*, Artistic (A), ClipArt (C), Product (P), and Real-world (R). Each domain is divided into six disjoint subsets with 10 classes for each in random order. 3) **ImageNet-Caltech-CI** contains ImageNet-1K and Caltech-256 with shared 84 classes. It consists of two tasks: ImageNet (1000)  $\rightarrow$  Caltech (84) and Caltech (256)  $\rightarrow$  ImageNet (84), where eight disjoint subsets of the target domain are constructed to contain 10 classes for each. Refer to the supplementary material for more details on the dataset construction.

**Implementation details.** We adopt SGD as the optimizer and the base learning rate is set to 0.001 with the batch size of 32. The number of incremental classes  $\gamma$  at each session is set to 10. In the early iterations, we identify multi-granularity class prototypes with the source model and then use the well-trained target model. For  $\mathcal{L}_{com}$ , we exponentially decrease the coefficient  $\mu_c$  as  $\mu_c^i = \mu_c^{i-1} e^{-\beta}$  at the  $i$ -th iteration, where initial  $\mu_c^0$  is set to 0.5 and  $\beta$  is set to 1e-4. Moreover, the stored exemplar  $n_r$  of each existing positive class in the memory bank is set to 10.

**Evaluation protocols.** We evaluate our method through two metrics: 1) **Final Accuracy**: the classification accuracy over all the classes at the final session. 2) **Session Accuracy**: the classification accuracy of each session to evaluate the ability of continual adaptation.

Table 1: Final accuracy (%) comparisons in the class-incremental scenario on Office-31-CI and ImageNet-Caltech-CI. U, CI, and SF respectively represent unsupervised, class-incremental, and source data-free. -B indicates the backbone is changed to ViT-B. \* indicates the result is derived from ProCA.

Method	U	CI	SF	Office-31-CI							ImageNet-Caltech-CI		
				A→D	A→W	D→A	D→W	W→A	W→D	Avg.	C→I	I→C	Avg.
ViT-B	✗	✗	✗	82.4	80.0	70.8	83.1	75.1	87.4	79.8	82.7	78.6	80.7
CIDA* (ECCV20)	✗	✓	✓	70.4	64.5	48.1	95.1	52.7	98.8	71.6	69.3	49.2	59.2
ProCA-B (ECCV22)	✓	✓	✗	93.4	91.9	73.0	98.3	77.6	99.2	88.9	91.6	84.0	87.8
PLUE (CVPR23)	✓	✗	✓	74.5	74.6	70.3	85.7	70.5	80.1	76.0	82.4	70.6	76.5
TPDS (IJCV23)	✓	✗	✓	78.1	74.6	71.1	90.3	69.7	91.9	79.3	85.0	68.0	76.5
LCFD (Arxiv24)	✓	✗	✓	51.6	53.9	48.3	61.2	44.4	86.8	57.7	77.4	66.9	72.2
DIFO (CVPR24)	✓	✗	✓	83.4	80.2	66.9	91.7	68.1	91.5	80.3	62.2	60.6	61.4
LEAD-B (CVPR24)	✓	✗	✓	92.3	92.2	76.8	98.1	76.3	100.0	89.3	89.2	53.0	71.1
GROTO (Ours)	✓	✓	✓	<b>99.4</b>	<b>99.0</b>	<b>81.3</b>	<b>99.0</b>	<b>81.3</b>	<b>98.1</b>	<b>93.0</b>	<b>92.5</b>	<b>85.1</b>	<b>88.8</b>

Table 2: Final accuracy (%) comparisons in the class-incremental scenario on Office-Home-CI.

Method	U	CI	SF	A→C	A→P	A→R	C→A	C→P	C→R	P→A	P→C	P→R	R→A	R→C	R→P	Avg.
				ViT-B	✗	✗	✗	53.2	77.7	82.1	69.1	76.6	78.7	67.8	50.8	82.1
CIDA* (ECCV20)	✗	✓	✓	32.2	45.9	49.1	36.5	48.6	46.6	51.6	33.5	59.0	64.0	38.0	65.1	47.5
ProCA-B (ECCV22)	✓	✓	✗	60.5	88.0	92.9	83.3	89.7	91.0	81.7	57.1	94.1	86.9	55.8	92.9	81.2
PLUE (CVPR23)	✓	✗	✓	28.8	67.9	72.5	60.5	67.5	73.4	59.6	29.2	74.2	61.2	37.6	72.6	58.8
TPDS (IJCV23)	✓	✗	✓	40.5	63.5	69.0	64.7	67.3	68.7	63.8	40.8	71.5	68.2	29.4	65.8	59.4
DIFO (CVPR24)	✓	✗	✓	44.7	62.6	61.5	54.1	59.8	61.6	53.7	37.6	65.2	58.4	43.3	57.5	55.0
LEAD-B (CVPR24)	✓	✗	✓	33.9	81.8	86.9	76.1	82.4	84.8	74.0	19.2	87.3	79.7	15.2	84.3	67.1
LCFD (Arxiv24)	✓	✗	✓	54.7	72.2	79.6	67.7	72.3	76.6	67.2	52.6	79.6	71.5	55.3	76.3	68.8
GROTO (Ours)	✓	✓	✓	<b>65.7</b>	<b>86.4</b>	<b>89.7</b>	<b>85.8</b>	<b>86.3</b>	<b>90.0</b>	<b>86.0</b>	<b>67.1</b>	<b>90.1</b>	<b>86.9</b>	<b>66.2</b>	<b>89.3</b>	<b>82.5</b>

## 4.2 Comparisons with SOTA Methods

We compare GROTO with five types of methods: (1) source-only: ViT-B [6]; (2) class-incremental domain adaptation: CIDA [14]; (3) class-incremental unsupervised domain adaptation: ProCA [18]; (4) source-free unsupervised domain adaptation: PLUE [19], TPDS [29] and DIFO [31]; (5) source-free universal domain adaptation: LEAD [24] and LCFD [30].

The final accuracy results of GROTO and the compared methods are reported in Table 1 and Table 2, which give the following observations. 1) GROTO shows the superiority of final accuracy in all sub-tasks compared to other methods. 2) Compared to SFUDA methods [19, 29, 31], GROTO performs better. It demonstrates the importance of reducing negative transfer caused by source negative classes and adapting to new classes while retaining old knowledge in CI-SFUDA. 3) The CIDA [14] method uses the regularization on proxy-source samples to mitigate catastrophic forgetting in source-free domain adaptation. However, it overlooks the target-class biased learning caused by the source negative classes, limiting its effectiveness in CI-SFUDA. 4) The CI-UDA method (ProCA [18]) preserves old knowledge through the exemplar replay strategy. However, it relies on source data to deal with the domain alignment problem, which makes it difficult to satisfy the data privacy issues. 5) SF-UniDA methods [24, 30] effectively prevent target features from shifting toward similar source clusters outside the target label space. However, they perform even worse than ViT-B, which shows that only focusing on domain alignment leads

the model to overfit the new classes and disrupt old knowledge in CI-SFUDA.

The session accuracy comparisons of different methods are shown in Table 3. Since no old knowledge and catastrophic problem at the first session, the SF-UniDA method (LEAD [24]) performs well. Compared to them, the SFUDA method (DIFO [31]) achieves slightly lower performance, as it doesn’t account for interference from source classes unrelated to target classes. GROTO can perform best at the first incremental session, illustrating the effectiveness of the multi-granularity class prototype self-organization module. At later sessions, due to the absence of old-class instances, the model may forget the old knowledge when adapting to new classes, resulting in performance degradation. As shown in Figure 3, the models of other methods continually show significant drops in the average accuracy of 10 classes learned at session 1, but GROTO maintains stable performances, indicating that it is effective in mitigating the shocks of new classes to old knowledge.

## 4.3 Ablation Studies

**Loss and Module Ablations.** To examine the loss and module effectiveness of GROTO, we show the ablation results in Table 4. Compared to the source-only model (Exps.A), the final accuracy is improved with the introduction of  $\mathcal{L}_{rep}$ ,  $\mathcal{L}_{ptfs}$  or  $\mathcal{L}_{ptd}$ . Moreover, the final accuracy decreases when the HKPCM, PTFS, or PTD module is removed.

Target cumulative probability and source average similar-

Table 3: Session accuracy (%) comparisons in the class-incremental scenario on Office-31-CI and Office-Home-CI.

Method	U	CI	SF	Office-31-CI				Office-Home-CI						
				Session 1	Session 2	Session 3	Avg.	Session 1	Session 2	Session 3	Session 4	Session 5	Session 6	Avg.
CIDA* (ECCV20)	✗	✓	✓	85.5	79.1	71.6	78.7	57.9	53.6	51.8	50.1	49.6	47.5	51.8
ProCA-B (ECCV22)	✓	✓	✗	90.5	90.0	89.0	89.8	76.3	81.0	80.1	81.0	81.6	81.2	80.2
LCFD (Arxiv24)	✓	✗	✓	81.3	68.9	57.7	69.3	70.0	64.9	68.2	68.1	67.9	68.8	68.0
DIFO (CVPR24)	✓	✗	✓	82.0	66.8	80.3	76.4	77.2	37.1	47.9	51.4	51.7	55.0	53.4
LEAD-B (CVPR24)	✓	✗	✓	96.4	91.6	89.3	92.4	70.0	64.9	68.2	68.1	67.9	68.8	68.0
GROTO (Ours)	✓	✓	✓	<b>96.7</b>	<b>94.9</b>	<b>93.0</b>	<b>94.9</b>	<b>84.4</b>	<b>84.8</b>	<b>81.7</b>	<b>83.3</b>	<b>82.8</b>	<b>82.5</b>	<b>83.2</b>

Table 4: Ablations of losses (*i.e.*,  $\mathcal{L}_{rep}$ ,  $\mathcal{L}_{ptfs}$  and  $\mathcal{L}_{ptd}$ ) and modules (*i.e.*, HKPCM, PTFS and PTD) in GROTO. We show the final accuracy (%) on all the tasks of Office-31-CI.

Exps.	$\mathcal{L}_{rep}$	$\mathcal{L}_{ptfs}$	$\mathcal{L}_{ptd}$	Final Accuracy (%)						
				A→DA	→WD	→AD	→WW	→AW	→DAvg.	
A				82.4	80.0	70.8	83.1	75.1	87.4	79.8
B	✓			90.7	91.9	74.0	98.1	77.2	98.3	88.4
C	✓	✓		96.5	97.3	80.9	99.2	80.6	97.5	92.0
D	✓	✓	✓	<b>99.4</b>	<b>99.0</b>	<b>81.3</b>	99.0	<b>81.3</b>	98.1	<b>93.0</b>
GROTO w/o HKPCM				97.5	95.5	80.6	99.2	75.1	98.1	91.0
GROTO w/o PTFS				88.4	91.6	73.8	98.2	77.3	99.0	88.0
GROTO w/o PTD				96.5	97.3	80.9	99.2	80.6	97.5	92.0
GROTO				<b>99.4</b>	<b>99.0</b>	<b>81.3</b>	99.0	<b>81.3</b>	98.1	<b>93.0</b>

ity distribution of Office-31-CI (A→D) at the first session are shown in Figure 4. We can observe that both the positive-class ones are higher than the negative-class ones. In the left sub-figure, only depending on the model predictions to mine the positive classes leads to omissions of class “4” (pointed by the black arrow), resulting in training with the wrong pseudo-labels at new sessions. Based on this observation, the HKPCM module is proposed to prevent error accumulation due to the missing positive classes, and its effectiveness is verified through the ablation experiment of “GROTO w/o HKPCM” in Table 4.

In the experiment of only introducing  $\mathcal{L}_{rep}$  (Exps.B), the HKPCM module is used, but it relies on simple model predictions to generate pseudo labels for unlabeled target data. In the experiment of introducing  $\mathcal{L}_{rep}$  and  $\mathcal{L}_{ptfs}$  (Exps.C), we first mine the positive classes through the HKPCM module, and then generate pseudo labels through the PTFS module. With the comparison of these two experiments, we can observe the effectiveness of the PTFS module which provides reliable pseudo labels. The experiment “GROTO w/o PTFS” further validates the conclusion. In addition, we show the multi-granularity class prototype visualizations of partial classes on Office-31-CI (A→D), and the target feature distributions of different methods on Office-31-CI (D→A) in Figure 5. It can be seen that the coarse-grained prototypes represent the center of the feature distribution, while the fine-grained prototypes contain detailed information on the feature distribution. The combination of them can represent the shape of the feature distribution well. Moreover, Figure 5 shows that the source-

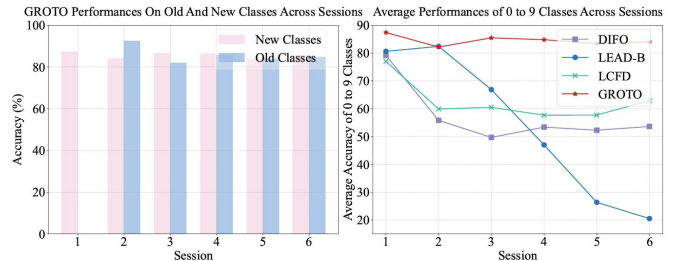


Figure 3: The accuracies on old and new classes of GROTO on Office-Home-CI (P→A), and the average accuracies of 0 to 9 classes for different methods across sessions on Office-Home-CI (P→A).

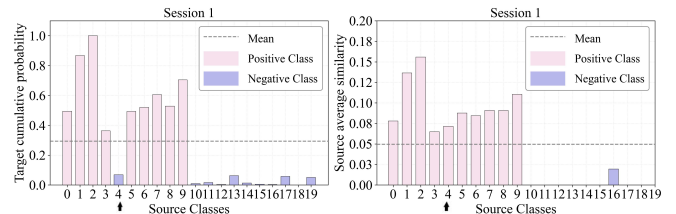


Figure 4: The target cumulative probability and source average similarity results at the first session on Office-31-CI (A→D). Only training data from 0 to 9 classes are provided at this session. Based on both distributions, we select classes with indices 0-9 as the positive classes at this session.

only model (ViT-B), ProCA-B, and LEAD-B mix the target features of similar classes. However, GROTO alleviates the disturbance of similar source-class knowledge to target-class representation learning, thus showing a more discriminative cluster distribution among different classes.

The experiments of introducing  $\mathcal{L}_{ptd}$  (Exps.D) and “GROTO w/o PTD” demonstrate that the PTD module improves the final accuracy. To investigate its impact on old-class knowledge, we visualize old-class and new-class features at the last session on Office-31-CI (A→D) as shown in Figure 6. GROTO without the PTD module (left sub-figure) incorrectly classifies old-class data to new ones in the top center part. Fewer old data are misclassified to new classes with the PTD module, thus improving the overall classification accuracy of old and new classes (93.8%→96.4%). It also proves that the PTD module effectively mitigates the problem of ex-

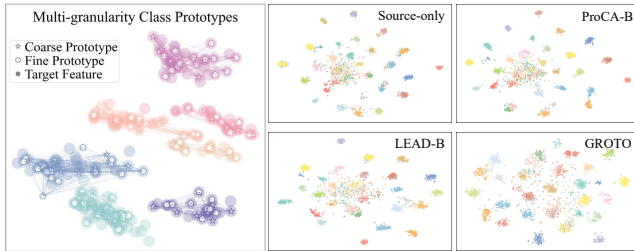


Figure 5: The multi-granularity class prototype visualizations of partial classes on Office-31-CI (A→D), and target feature distribution of source-only, ProCA-B, LEAD-B and GROTO methods on Office-31-CI (D→A).

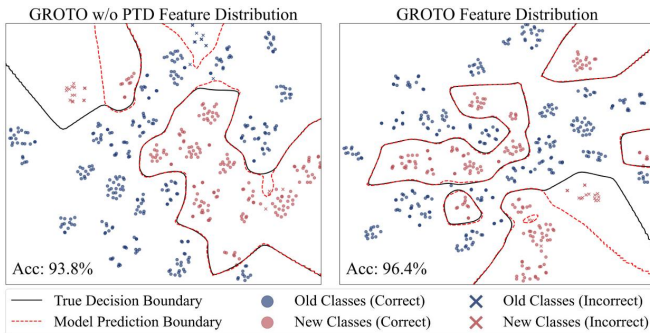


Figure 6: The feature distribution and decision boundary visualizations of “GROTO w/o PTD” and GROTO models on Office-31-CI (A→D). “GROTO w/o PTD” tends to incorrectly classify old-class data to new ones.

cessively focusing on new classes while forgetting old knowledge during the continual adaptation process.

**Hyper-parameter Ablations.** We explore the impacts of hyper-parameters in Table 5, indicating that GROTO has relatively stable performance with different values of  $\mu_c^0$  and  $\beta$ . The final accuracy is highest when the number of incremental classes  $\gamma$  is 13, but to ensure the experimental setup is consistent with ProCA, we chose 10 as the number of incremental classes for GROTO.

## 5 Conclusion

In this paper, we explore the class-incremental source-free unsupervised domain adaptation (CI-SFUDA) problem. To address it, we propose a novel Multi-Granularity Class Prototype Topology Distillation (GROTO) algorithm, which consists of two modules. (1) Multi-granularity class prototype self-organization: we mine the positive classes by modeling source similarity and target probability class accumulation distributions. Then we introduce the multi-granularity class prototypes to generate reliable pseudo-labels, thus promoting the target feature self-organization. (2) Prototype topology distillation: we construct the topological structures of feature manifolds with source and target prototypes, and perform the point-to-point cross-domain topology distillation to maintain

Table 5: Ablations of different hyper-parameters (i.e.,  $\gamma$ ,  $\mu_c^0$ ,  $\beta$  and  $n_r$ ) on ImageNet-Caltech-CI.

$\gamma$	Avg.	$\mu_c^0$	Avg.	$\beta$	Avg.	$n_r$	Avg.
9	87.5	0.2	88.5	1e-5	88.7	1	83.0
10	88.8	0.5	<b>88.8</b>	5e-5	88.8	5	86.2
11	87.8	0.6	87.5	1e-4	<b>88.8</b>	10	<b>88.8</b>
12	87.3	0.7	85.4	5e-4	87.3	15	88.7
13	<b>89.1</b>	0.8	88.0	1e-3	88.3	20	88.7

consistency of the source knowledge of all classes and the gradually accumulated target knowledge. Therefore, we can continually mitigate the disturbances of new target knowledge to old ones. Extensive experiments demonstrate the effectiveness of GROTO on three public datasets in handling CI-SFUDA, and it achieves state-of-the-art performances.

## References

- [1] Zhangjie Cao, Mingsheng Long, Jianmin Wang, and Michael I Jordan. Partial transfer learning with selective adversarial networks. In *Proceedings of the IEEE conference on computer vision and pattern recognition*, pages 2724–2732, 2018. 1
- [2] Zhangjie Cao, Kaichao You, Mingsheng Long, Jianmin Wang, and Qiang Yang. Learning to transfer examples for partial domain adaptation. In *Proceedings of the IEEE/CVF conference on computer vision and pattern recognition*, pages 2985–2994, 2019. 1
- [3] Xi Chen, Haosen Yang, Huicong Zhang, Hongxun Yao, and Xiatian Zhu. Uncertainty-aware pseudo-label filtering for source-free unsupervised domain adaptation. *Neurocomputing*, 575: 127190, 2024. 1, 2
- [4] Ziyang Chen, Yongsheng Pan, and Yong Xia. Reconstruction-driven dynamic refinement based unsupervised domain adaptation for joint optic disc and cup segmentation. *IEEE Journal of Biomedical and Health Informatics*, 27(7):3537–3548, 2023. 1
- [5] Matthias De Lange, Rahaf Aljundi, Marc Masana, Sarah Parisot, Xu Jia, Aleš Leonardis, Gregory Slabaugh, and Tinne Tuytelaars. A continual learning survey: Defying forgetting in classification tasks. *IEEE transactions on pattern analysis and machine intelligence*, 44(7):3366–3385, 2021. 5
- [6] Alexey Dosovitskiy, Lucas Beyer, Alexander Kolesnikov, Dirk Weissenborn, Xiaohua Zhai, Thomas Unterthiner, Mostafa Dehghani, Matthias Minderer, Georg Heigold, Sylvain Gelly, et al. An image is worth 16x16 words: Transformers for image recognition at scale. *arXiv preprint arXiv:2010.11929*, 2020. 6
- [7] Xinyuan Gao, Yuhang He, Songlin Dong, Jie Cheng, Xing Wei, and Yihong Gong. Dkt: Diverse knowledge transfer transformer for class incremental learning. In *Proceedings of the IEEE/CVF Conference on Computer Vision and Pattern Recognition*, pages 24236–24245, 2023. 2
- [8] Xinyuan Gao, Songlin Dong, Yuhang He, Xing Wei, and Yihong Gong. Ceat: Continual expansion and absorption transformer for non-exemplar class-incremental learning. *arXiv preprint arXiv:2403.06670*, 2024. 2



- [9] Gregory Griffin, Alex Holub, and Pietro Perona. Caltech-256 object category dataset, 2007. *CIT Technical Report*, 7694, 2020. 5
- [10] Yuhang He, Yingjie Chen, Yuhan Jin, Songlin Dong, Xing Wei, and Yihong Gong. Dyson: Dynamic feature space self-organization for online task-free class incremental learning. In *Proceedings of the IEEE/CVF Conference on Computer Vision and Pattern Recognition*, pages 23741–23751, 2024. 2
- [11] Minsoo Kang, Jaeyoo Park, and Bohyung Han. Class-incremental learning by knowledge distillation with adaptive feature consolidation. In *Proceedings of the IEEE/CVF conference on computer vision and pattern recognition*, pages 16071–16080, 2022. 2
- [12] Nazmul Karim, Niluthpol Chowdhury Mithun, Abhinav Rajvanshi, Han-pang Chiu, Supun Samarasekera, and Nazanin Rahnavard. C-sfda: A curriculum learning aided self-training framework for efficient source free domain adaptation. In *Proceedings of the IEEE/CVF Conference on Computer Vision and Pattern Recognition*, pages 24120–24131, 2023. 1, 2
- [13] Prannay Khosla, Piotr Teterwak, Chen Wang, Aaron Sarna, Yonglong Tian, Phillip Isola, Aaron Maschiot, Ce Liu, and Dilip Krishnan. Supervised contrastive learning. *Advances in neural information processing systems*, 33:18661–18673, 2020. 4
- [14] Jogendra Nath Kundu, Rahul Mysore Venkatesh, Naveen Venkat, Ambareesh Revanur, and R Venkatesh Babu. Class-incremental domain adaptation. In *Computer Vision–ECCV 2020: 16th European Conference, Glasgow, UK, August 23–28, 2020, Proceedings, Part XIII 16*, pages 53–69. Springer, 2020. 2, 6
- [15] Kunchi Li, Jun Wan, Sergio Escalera, Zhen Lei, and Shan Yu. Effective decision boundary learning for class incremental learning. 2023. 5
- [16] Jian Liang, Dapeng Hu, and Jiashi Feng. Do we really need to access the source data? source hypothesis transfer for unsupervised domain adaptation. In *International conference on machine learning*, pages 6028–6039. PMLR, 2020. 2
- [17] Jian Liang, Dapeng Hu, Jiashi Feng, and Ran He. Umad: Universal model adaptation under domain and category shift. *arXiv preprint arXiv:2112.08553*, 2021. 2
- [18] Hongbin Lin, Yifan Zhang, Zhen Qiu, Shuaicheng Niu, Chuang Gan, Yanxia Liu, and Mingkui Tan. Prototype-guided continual adaptation for class-incremental unsupervised domain adaptation. In *European Conference on Computer Vision*, pages 351–368. Springer, 2022. 1, 2, 5, 6
- [19] Mattia Litrico, Alessio Del Bue, and Pietro Morerio. Guiding pseudo-labels with uncertainty estimation for source-free unsupervised domain adaptation. In *Proceedings of the IEEE/CVF Conference on Computer Vision and Pattern Recognition*, pages 7640–7650, 2023. 6
- [20] Ismail Nejjar, Qin Wang, and Olga Fink. Dare-gram: Unsupervised domain adaptation regression by aligning inverse gram matrices. In *Proceedings of the IEEE/CVF conference on computer vision and pattern recognition*, pages 11744–11754, 2023. 1
- [21] Shuaicheng Niu, Jiaxiang Wu, Yifan Zhang, Yaofu Chen, Shijian Zheng, Peilin Zhao, and Mingkui Tan. Efficient test-time model adaptation without forgetting. In *International conference on machine learning*, pages 16888–16905. PMLR, 2022. 1
- [22] Sanqing Qu, Guang Chen, Jing Zhang, Zhijun Li, Wei He, and Dacheng Tao. Bmd: A general class-balanced multicentric dynamic prototype strategy for source-free domain adaptation. In *European conference on computer vision*, pages 165–182. Springer, 2022. 1, 2
- [23] Sanqing Qu, Tianpei Zou, Florian Röhrbein, Cewu Lu, Guang Chen, Dacheng Tao, and Changjun Jiang. Upcycling models under domain and category shift. In *Proceedings of the IEEE/CVF Conference on Computer Vision and Pattern Recognition*, pages 20019–20028, 2023. 1, 2
- [24] Sanqing Qu, Tianpei Zou, Lianghua He, Florian Röhrbein, Alois Knoll, Guang Chen, and Changjun Jiang. Lead: Learning decomposition for source-free universal domain adaptation. In *Proceedings of the IEEE/CVF Conference on Computer Vision and Pattern Recognition*, pages 23334–23343, 2024. 1, 2, 6
- [25] Sylvestre-Alvise Rebuffi, Alexander Kolesnikov, Georg Sperl, and Christoph H Lampert. icarl: Incremental classifier and representation learning. In *Proceedings of the IEEE conference on Computer Vision and Pattern Recognition*, pages 2001–2010, 2017. 2
- [26] Arun Reddy, William Paul, Corban Rivera, Ketul Shah, Celso M de Melo, and Rama Chellappa. Unsupervised video domain adaptation with masked pre-training and collaborative self-training. In *Proceedings of the IEEE/CVF Conference on Computer Vision and Pattern Recognition*, pages 18919–18929, 2024. 1
- [27] Olga Russakovsky, Jia Deng, Hao Su, Jonathan Krause, Sanjeev Satheesh, Sean Ma, Zhiheng Huang, Andrej Karpathy, Aditya Khosla, Michael Bernstein, et al. Imagenet large scale visual recognition challenge. *International journal of computer vision*, 115:211–252, 2015. 5
- [28] Kate Saenko, Brian Kulis, Mario Fritz, and Trevor Darrell. Adapting visual category models to new domains. In *Computer Vision–ECCV 2010: 11th European Conference on Computer Vision, Heraklion, Crete, Greece, September 5–11, 2010, Proceedings, Part IV 11*, pages 213–226. Springer, 2010. 5
- [29] Song Tang, An Chang, Fabian Zhang, Xiatian Zhu, Mao Ye, and Changshui Zhang. Source-free domain adaptation via target prediction distribution searching. *International journal of computer vision*, 132(3):654–672, 2024a. 6
- [30] Song Tang, Wenxin Su, Mao Ye, Jianwei Zhang, and Xiatian Zhu. Unified source-free domain adaptation. *arXiv preprint arXiv:2403.07601*, 2024b. 1, 2, 6
- [31] Song Tang, Wenxin Su, Mao Ye, and Xiatian Zhu. Source-free domain adaptation with frozen multimodal foundation model, 2024c. 6
- [32] Xiaoyu Tao, Xinyuan Chang, Xiaopeng Hong, Xing Wei, and Yihong Gong. Topology-preserving class-incremental learning. In *Computer Vision–ECCV 2020: 16th European Conference, Glasgow, UK, August 23–28, 2020, Proceedings, Part XIX 16*, pages 254–270. Springer, 2020. 2
- [33] Hemanth Venkateswara, Jose Eusebio, Shayok Chakraborty, and Sethuraman Panchanathan. Deep hashing network for unsupervised domain adaptation. In *Proceedings of the IEEE conference on computer vision and pattern recognition*, pages 5018–5027, 2017. 5

- [34] Yue Wu, Yinpeng Chen, Lijuan Wang, Yuancheng Ye, Zicheng Liu, Yandong Guo, and Yun Fu. Large scale incremental learning. In *Proceedings of the IEEE/CVF conference on computer vision and pattern recognition*, pages 374–382, 2019. [2](#), [5](#)
- [35] Kai Zhu, Wei Zhai, Yang Cao, Jiebo Luo, and Zheng-Jun Zha. Self-sustaining representation expansion for non-exemplar class-incremental learning. In *Proceedings of the IEEE/CVF Conference on Computer Vision and Pattern Recognition*, pages 9296–9305, 2022. [2](#)